Polymer Chemistry

Radical Free Crosslinking of Direct-Write 3D Printed Hydrogels Through a Base Catalyzed Thiol-Michael Reaction

Journal:	*Polymer Chemistry*
Manuscript ID	PY-ART-06-2019-000953.R1
Article Type:	Paper
Date Submitted by the Author:	22-Aug-2019
Complete List of Authors:	Berry, Danielle; University of Texas at Dallas, Chemistry and Biochemistry Diaz, Brisa; University of Texas at Dallas, Chemistry and Biochemistry Durand-Silva, Alejandra; University of Texas at Dallas, Chemistry and Biochemistry Smaldone, Ronald; University of Texas at Dallas, Chemistry and Biochemistry

SCHOLARONE™
Manuscripts

ARTICLE

Radical Free Crosslinking of Direct-Write 3D Printed Hydrogels Through a Base Catalyzed Thiol-Michael Reaction

Danielle R. Berry,[a] Brisa K. Díaz,[a] Alejandra Durand-Silva,[a] and Ronald A. Smaldone*[a]

In this work we describe a method of fabricating 3D printed hydrogels which are mechanically stabilized without the use of potentially cytotoxic radical chemistry. To achieve this, we utilized a thiol-Michael reaction catalyzed by basic (pH 8.2) phosphate buffered saline (PBS) between diacrylated Pluronic F127 and multifunctional thiol crosslinkers. We showed that the print resolution could be conserved due to stabilization of Pluronic micelles as a result of the ionic strength of the buffer. These hydrogels exhibited high stretchability (~750%) as well as tunable mechanical properties. We demonstrated that micelle based free standing 3D objects can be fabricated through non-radical pathways by stabilizing the micelles in solutions with increased ionic strength.

Introduction

Hydrogels are a class of materials comprised of physically or chemically crosslinked polymers that are capable of absorbing large amounts of water.[1–4] Hydrogels are inherently soft materials, and various strategies have been employed to control their mechanical properties including the use of moveable crosslinks (slide-ring gels),[5–8] dual crosslinking networks,[9–11] the incorporation of nanocomposite fillers,[12–14] metal coordination linkages,[15,16] and micelle crosslinking.[17–19] By incorporating dynamic interactions into the hydrogel network, energy from an external force can be more easily dissipated throughout the gel, ultimately enhancing the toughness of the material. Hydrogels have found applications in agriculture,[20] sensors,[21–23] and regenerative medicine.[24–26] Hydrogels are excellent candidates for biomedical applications, specifically tissue engineering, given their biocompatiblity, ability to provide environments facilitating cell proliferation, tunable mechanical properties, and 3D structure.[27]

Developing new techniques for hydrogel fabrication that are compatible with 3D printing has been a major source of research as the custom production of these materials is critical to their use in many medical and biological applications.[28] Previous studies have demonstrated the fabrication of hydrogels with complex 3D structures *via* direct write 3D-printing from shear-thinning precursors.[29–33] Pluronics, a class of ABA triblock co-polymers, are often chosen for this method of printing due to their shear-thinning behavior.[34–36] 3D

printed Pluronics will readily hold their shape after printing, but can be easily deformed owing to the non-covalent nature of their assembly.[37] To improve the mechanical strength, and dimensional stability of the 3D printed shapes after curing,
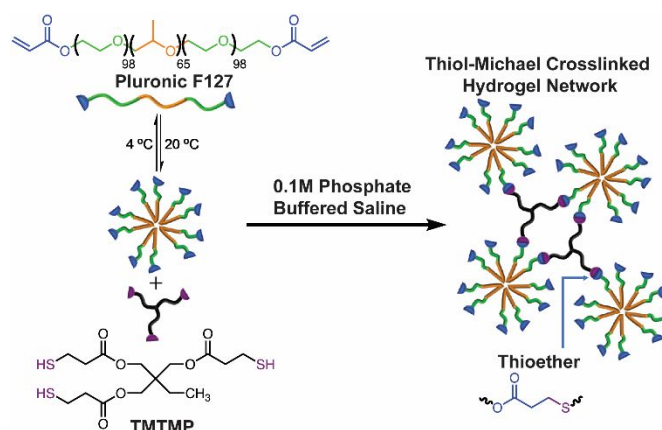
Scheme 1. Illustration of thiol-Michael crosslinking in micellar hydrogels.

acrylate endgroups can be added to these polymers which allows for the polyether micelles to be crosslinked through radical polymerization. For example, a report by Wu, *et. al.* used diacrylated Pluronic F127 (DAP127) as a support gel along with a "fugitive ink" to allow for direct-write printing of 3D structures with internal vascularization.[32] DAP127 has also been used to fabricate free-standing structures without the use of a support bath. In our recent work, we developed a 3D printed hydrogel whose shear-thinning properties could be mechanically stabilized through the addition of chitosan to the DAP127 formulation and covalently crosslinked using radical polymerization, for the removal of heavy metal pollutants from water.[38] However, these examples, and many others

[a.] *Department of Chemistry and Biochemistry, The University of Texas at Dallas, 800 W. Campbell Rd, Richardson, Texas 75080, USA. Email: ronald.smaldone@utdallas.edu*
† Footnotes relating to the title and/or authors should appear here.
Electronic Supplementary Information (ESI) available

utilize potentially toxic photo-initiators and exposure to UV light, both of which are harmful to cells.[39,40] A previous study by Williams, *et. al.* demonstrated the cytotoxicity of three commonly used photo-initiators (Irgacure 2959, 184, and 651) against six cell lines.[41] In this study, Irgacure 2959 was found to be the least toxic of the three initiators, and it has since been used for UV crosslinking of materials for biomedical applications.[42,43] Although this photo-initiator is less toxic in comparison, it still leads to cell death and limits the use of these materials in biomedical applications. For this reason, we have chosen to investigate non-radical methods of covalently crosslinking hydrogels after direct-write 3D printing.

To improve the biocompatibility of mechanically stable 3D printed objects, we chose to investigate the thiol-Michael addition for the crosslinking of Pluronic based materials. Although the thiol-Michael addition has been widely employed in the formation of hydrogels due to its mild reaction conditions and "click chemistry" characteristics,[44] it has found little use in direct-write 3D printing. One of the main challenges associated with direct-write printing is maintaining the resolution of the printed object while effectively crosslinking the deposited material. Radical polymerization has remained a prevalent curing technique for direct-write printed hydrogels because it occurs quickly, and requires minimal disturbance of the uncured object. Here, we demonstrate a method of simultaneously crosslinking hydrogels in basic buffer solutions while maintaining the three-dimensionally printed structure through enhanced micelle stability. The hydrogel structures are stabilized by the presence of sodium or potassium chloride in the buffer which drastically limits the dissolution or deformation of the un-crosslinked polymers in solution during the curing process. We achieved this through a base catalyzed thiol-Michael reaction, which was used to cure formulations of DAP127 and a multi-arm thiol crosslinker to fabricate 3D printed hydrogels with minimal dissolution of the hydrogel in the appropriate conditions (Scheme 1).

Experimental

General Experimental

All chemicals were used as received without further purification. Pluronic F127 (M_w 12,500) was purchased from Spectrum Chemical Corporation, New Brunswick, NJ, USA. Acryloyl chloride was purchased from Alfa Aesar, Haverhill, MA, USA. Trimethylolpropane tris(3-mercaptopropionate) (TMTMP) and Pentaerythritol tetrakis(3-mercaptopropionate) (PETMP) were purchased from TCI America, Portland, OR, USA. Dichloromethane, diethyl ether, and triethylamine were purchased from Fisher Chemical, Hampton, NH, USA. ^{1}H NMR spectra were obtained on a Bruker Avance III HD 600 MHz spectrometer.

Synthesis of Diacrylated Pluronic F127 (DAP127)

DAP127 was synthesized according to our previous work.[38] Pluronic F127 (12.5 g, 1 mmol) was dissolved in anhydrous dichloromethane (50 mL) and cooled to 0 °C. Triethylamine

(0.61 g, 6 mmol) was added and the solution was stirred for 10 min. Acryloyl chloride (0.54 g, 6 mmol) was added dropwise, and the reaction was stirred for 24 h. The crude product was extracted using dichloromethane (200 mL) and washed with deionized water (50 mL), saturated aqueous sodium bicarbonate (50 mL) and again with deionized water (50 mL). The organic phase was collected and dried over anhydrous sodium sulfate, and the solvent was removed under reduced pressure. The resulting solid was dissolved in dichloromethane (50 mL), cooled in an ice bath, and precipitated by the addition of diethyl ether. The final product was collected by filtration as a white solid and dried at 40 ºC under dynamic vacuum for 24 h. Yield 10.2 g, 81.6%. ^{1}H NMR (600 MHz, DMSO-d_6) δ 6.34 (d, J = 12 Hz, -CH$_2$), 6.2 (dd, J = 9, 12 Hz, -CH), 5.97 (d, J = 9 Hz, -CH$_2$), 3.56-3.44 (br, -OCHCH$_2$O-, -OCH$_2$CH$_2$O-), 1.04 (s, -CH$_3$).

Preparation of Thiol-Michael Crosslinked Hydrogels

Hydrogel compositions (Table S1) were prepared as follows. DAP127 was dissolved in deionized water at 4 °C using a magnetic stir bar. After the polymer was completely dissolved, TMTMP or PETMP was added and the mixtures were stirred vigorously, resulting in opaque solutions due to the decreased solubility of the crosslinkers in water at low temperatures. After 5 h, the solutions were kept at 4 °C without stirring to allow any bubbles to subside. The viscous hydrogel solutions were then transferred to a 60 mL syringe and kept at rt for 3 h over which time the solution became transparent.

Preparation of Control DAP Hydrogels

DAP127 was dissolved in deionized water at 4 °C using a magnetic stir bar. After the polymer was completely dissolved, Irgacure 754 was added, and the solution was stirred vigorously resulting in a transparent solution. After 5 h, the solution was kept at 4 °C without stirring to allow any bubbles to subside. The viscous solution was then transferred to a 60 mL syringe and kept at rt for 3 h before printing.

Direct Write 3D Printing of Hydrogels

All gel samples were prepared fresh before printing. The DAP127 formulations were 3D printed using a Printrbot 3D printer (Printrbot, Lincoln, CA, USA) modified with a paste extruder attachment and using the open source slicing software Cura (Ultimaker). Dogbones were printed according to the ISO 37-4 standard for tensile testing and cylinders with a diameter of 10 mm and thickness of 8 mm for compression testing. All samples were printed on a glass slide fixed to the printer bed for ease of transfer to curing solutions. The full printing parameters are outlined in the supplementary information (Table S2).

Post-Curing of Thiol-Michael Crosslinked Hydrogels and Control DAP127 Hydrogels

Printed hydrogels were incubated at 37 °C for 72 h or submerged in buffer solutions prepared with varying pH and

molarity (Table S3) for 24 h (Figure 1). Printed control DAP127 hydrogels were cured in a UV oven at 365 nm for 6 h, removed, and equilibrated in 0.1 M PBS for 24 h.

Quantification of Hydrogel Swelling

Printed hydrogel dogbone samples were submerged in deionized water for 24 h and allowed to dry at room temperature under ambient pressure for three days. The dry weight of each sample was measured, and the samples were then soaked in PBS solutions of varying concentration (Figure 3). Each sample was weighed after equilibration for 24 h and swelling was calculated as:

$$\left(\frac{W_s - W_d}{W_d}\right) * 100 = \% \text{ swelling by weight}$$

where W_s is the swollen weight of the sample, and W_d is the dry weight of the sample.

Mechanical Testing

All mechanical tests were performed on an Instron 5848 Micro Tester (Illinois Tool Works, Inc, Norwood, MA, USA). Tensile testing was performed on dogbone samples after curing for 24 h in 0.1 M PBS with a 50 N load cell at a rate of 20 mm/min. Sand paper was placed between the gel sample and clamps to avoid slippage of the sample. Compression samples were tested at 24, 72, and 120 h with a 1 kN load cell at a rate of 2 mm/min. Samples were tested in triplicate and error bars were calculated as the standard deviation of the three replicates.

Dimensional Stability and Shape Recovery Tests

To evaluate dimensional stability, dogbone samples were measured directly after printing and after soaking for 24 h in 0.1 M PBS. For shape recovery, the initial lengths of tensile samples of DAP127/TMTMP$_{0.67}$ were measured. The samples were then elongated to 400% strain, measured, and recovered at room temperature, incubation at 37 °C, and in PBS (pH 8.2). After 22 h, the samples lengths were measured. The percent size increase for both tests was calculated as:

$$\left(\frac{L_f - L_i}{L_i}\right) * 100 = \% \text{ size increase}$$

Where L_f is the final length of the sample and L_i is the initial length. Samples were tested in triplicate and error bars were calculated as the standard deviation of the three replicates.

Results and discussion

We mixed TMTMP with DAP127 in a 1:1 ratio by functional group (DAP127-TMTMP$_{0.67}$) and attempted to cure the thiol-Michael gels using various conditions including incubation, or under basic pH using potassium phosphate (KP) and PBS buffers (pH 8.0 and 8.2 respectively), two common buffers used in the cultivation of cells and tissues. Pluronic F127 behaves as a thermoresponsive hydrogel due to micelle formation at concentrations greater than 20 wt% at

room temperature.[45] A study by Su, *et. al.* reported the increased stability of Pluronic micelles in aqueous salt solutions compared to pure water.[46] It was found that with respect to cations, Na$^+$ has a greater improvement on micelle stability than K$^+$, while anionic stabilization effects follow the Hofmeister series (Cl$^-$ >Br$^-$ > I$^-$) in potassium halides. By exploiting these properties, we were able to limit dissolution of the printed DAP gels by using PBS (which contains both NaCl and KCl, thereby aiding in micelle stabilization), while simultaneously crosslinking the DAP127 due to the basic pH of the buffer. PBS showed retention of the 3D structure while samples in KP buffer (which does not contain NaCl or KCl) eventually dissolved (Figure 1) indicating that basic pH alone is not enough to stabilize and crosslink the hydrogels while retaining print resolution.
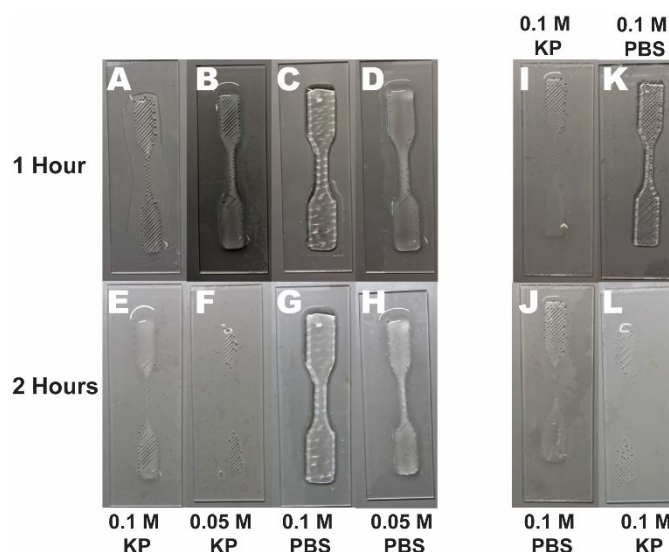

Figure 1. DAP127-TMTMP$_{0.67}$, cured in 0.1 M potassium phosphate (KP) buffer (pH 8.0), 0.05 M KP buffer, 0.1 M phosphate buffered saline (PBS, pH 8.2), and 0.05 M PBS, for 1 h (**A-D**) and 2 h (**E-H**). DAP127-TMTMP$_{0.67}$, cured in 0.1 M KP buffer for 1 h (**I**), followed by 1 h in 0.1 M PBS (**J**), and DAP127-TMTMP$_{0.67}$ cured in 0.1 M PBS for 1 h (**K**) followed by 1 h in 0.1 M KP buffer (**L**).

We identified 0.1 M PBS as the best candidate for post-fabrication treatment of the hydrogels, as it was the only solution to result in a free-standing 3D object (Figure 1 C, G). The concentration of salt also plays a large role in the diffusion of water into the gel, limiting its swelling behavior. As the concentration of ions in solution increases, the hydrophobic interactions within the polypropylene oxide (PPO) block are strengthened leading to a more compact 3D structure (Figure 2A). It was also observed that the swelling ratios for control DAP127 did not vary as drastically as that of the thiol-Michael gel. This may be due to a higher crosslinking density of the material, leading to a restriction in the swelling behavior (Figure 2A).
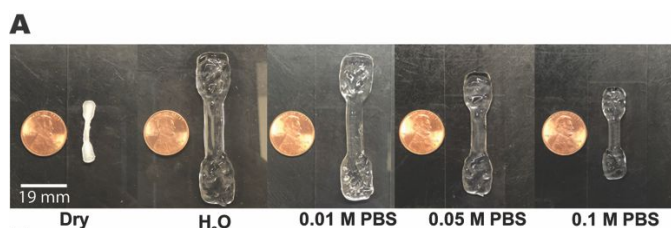
Figure 2. A, Optical images of DAP127-TMTMP$_{0.67}$ swollen in increasing concentrations of PBS (pH 8.2), and **B**, table of swelling percent by weight of DAP127-TMTMP$_{0.67}$ hydrogels in increasing concentrations of PBS.

After identifying the appropriate crosslinking conditions, the various formulations of printed DAP gels were soaked in 0.1 M PBS. After 24 h formulations DAP127-TMTMP$_1$ and DAP127-TMTMP$_{0.67}$ formed freestanding objects, where DAP127-TMTMP$_{0.33}$ dissolved. This indicated that a minimum ratio of 1:1 thiol to acrylate functional group was required for gelation. After soaking, the crosslinked gels were stretched by hand. DAP127-TMTMP$_1$ began to crumble at the surface (Figure S2 A) while DAP127-TMTMP$_{0.67}$ remained smooth after stretching. The poor mechanical properties of DAP127-TMTMP$_1$ may be attributed to insufficient crosslinking of the material in the presence of excess thiol functional groups. Based on this result, a 1:1 ratio of functional groups was chosen for testing crosslinking conditions with PETMP.

Next we evaluated the mechanical properties by tensile and compression testing. Formulations of DAP127-TMTMP$_{0.67}$ and DAP127-PETMP$_{0.5}$ were used for testing. The TMTMP crosslinker showed excellent strain tolerance with maximum elongation up to ~750% (Figure 3). PETMP, while still elastic, did not perform as well as the three-armed TMTMP cross-linker. Similar to the DAP127-TMTMP$_1$ formulation, the PETMP gel exhibited inhomogeneity along the gels surface as stretching occurred (Figure S2 B), resulting in lower tensile strength (Figure 3 C). DAP127 control gels were unable to be tested by this method as they were too brittle and broke under the force of the clamp.
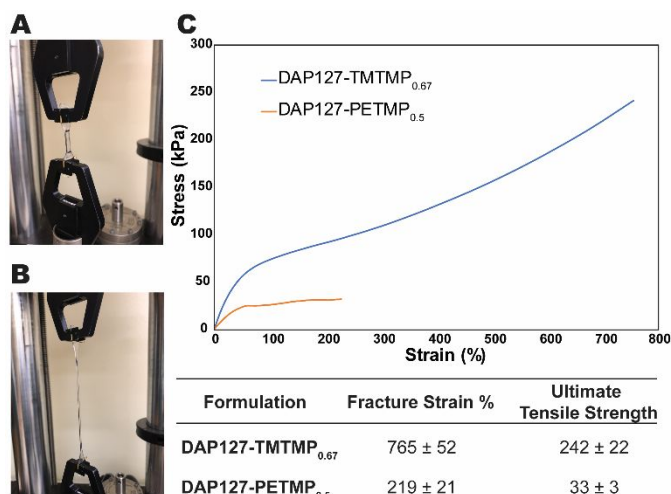

Figure 3. Optical image of tensile testing of DAP127-TMTMP$_{0.67}$ **A**, before stretching and **B**, under strain. **C**, stress-strain curves, fracture strain at maximum elongation, and ultimate tensile strength at break of DAP127-TMTMP$_{0.67}$ and DAP127-PETMP$_{0.5}$.

We also evaluated the recovery of DAP127-TMTMP$_{0.67}$ and found that the material recovered within 7% of the original length after 22 h in 0.1 M PBS (Figure 4). Previous reports have shown micelle based materials to have shape memory properties,[47,48] however, this hydrogel also recovered after 22 h at room temperature and when incubated at 37 °C (Figure S3), demonstrating that the material behaves elastically and will recover regardless of the stimulus.
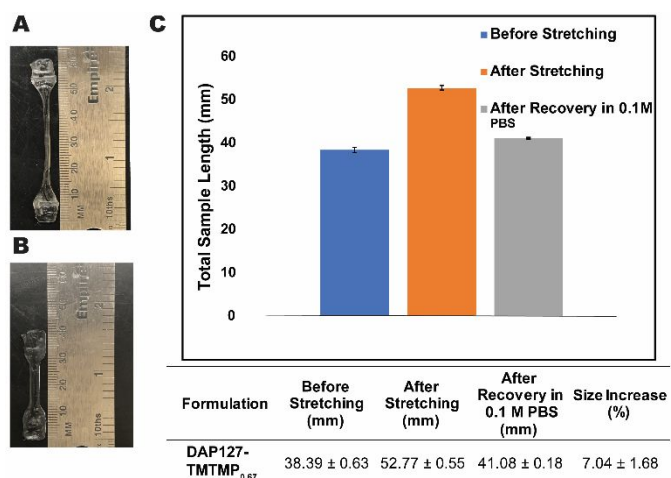

Figure 4. Optical image of **A**, DAP127-TMTMP$_{0.67}$ directly after stretching and **B**, after recovery for 24 h in PBS. **C**, values of total sample lengths before and after stretching, and after recovery.

To compare the mechanical properties of the thiol-Michael gels to the control DAP127 gel crosslinked using radicals, compression testing was performed and compressive moduli were calculated for each sample over a period of five days (Figure 5). In these tests, we can also see the influence of micelle stabilization on the mechanical properties of the control DAP127 gel. We hypothesize that the increased mechanical strength can be attributed to the slow/continuous diffusion of salts into the gel, resulting in increased micelle stabilization over time.[49] In the thiol-Michael crosslinked gels,

we observed a decrease in mechanical properties over time. This decrease in modulus is likely attributed to the hydrolysis of esters in the system. A previous report described an increased hydrolysis rate for esters with neighboring sulfur atoms, which is the adduct formed through the thiol-Michael addition in this work.[50] Because there are no sulfur atoms present in the control DAP127 gel, the hydrolysis rate is likely decreased, therefore we do not see a resultant change in mechanical properties. The compression tests also illustrate the tunable mechanical properties of these gels, which cannot easily be achieved at a constant polymer concentration using conventional radical polymerization. This becomes increasingly important when considering biomedical applications. According to values outlined in a review of engineered hydrogels,[51] the control DAP127 gels approach the modulus range of cartilage (~500 kPa), while DAP127-PETMP$_{0.5}$ and DAP127-TMTMP$_{0.67}$ fall between tendon and cartilage (30-500 kPa) by compression and reach values as soft as skin and muscles (10-30 kPa) by tension (Figure S4).
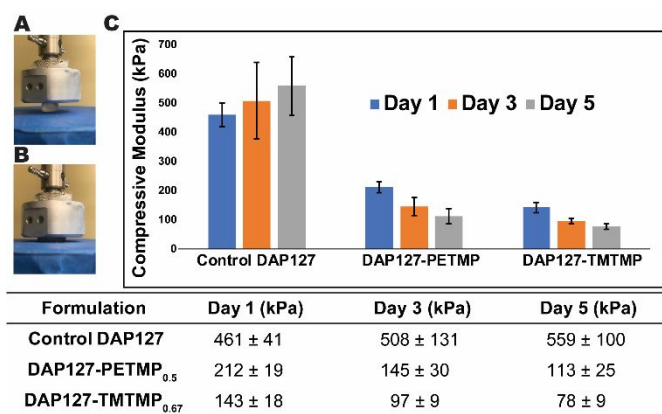

Formulation	Day 1 (kPa)	Day 3 (kPa)	Day 5 (kPa)
Control DAP127	461 ± 41	508 ± 131	559 ± 100
DAP127-PETMP$_{0.5}$	212 ± 19	145 ± 30	113 ± 25
DAP127-TMTMP$_{0.67}$	143 ± 18	97 ± 9	78 ± 9

Figure 5. Optical image of **A**, DAP127-PETMP$_{0.5}$ before compression and **B**, under compression. **C**, compressive moduli of control DAP127, DAP127-PETMP$_{0.5}$, and DAP127-TMTMP$_{0.67}$ after 1, 3, and 5 days in 0.1 M PBS.

Conclusions

We have demonstrated how the thiol-Michael addition can be used as a tool for the post-print curing of ABA type tri-block co-polymers by exploiting their micelle formation. The use of this non-radical reaction eliminated the need for potentially cytotoxic photo-initiators and UV light in the formation of hydrogels. By varying the crosslinker as well as the curing conditions, we are able to tune the mechanical strength to match that of various organ tissue types without sacrificing 3D printability or resolution of the printed parts. We demonstrated that we could achieve high strain tolerance (up to ~750%) as well as the ability to recover the original shape of the materials. We believe that consideration of the ionic strength of the aqueous post-print curing solutions could be used as a general strategy to open up the use of other crosslinking reactions with micelle-based systems. Future studies will be aimed at using this methodology to expand the

toolbox of chemical bond formations that are compatible with direct write 3D printing.

Conflicts of interest

The authors have no conflicts to declare.

Acknowledgements

Notes and references

1 E. M. Ahmed, *J. Adv. Res.*, 2015, **6**, 105–121.
2 A. J. Guerra, H. Lara-Padilla, M. L. Becker, C. A. Rodriguez and D. Dean, *Curr. Drug Targets*, 2019, **20**, 823–838.
3 A. K. Means and M. A. Grunlan, *ACS Macro Lett.*, 2019, **8**, 705–713.
4 P. Nezhad-Mokhtari, M. Ghorbani, L. Roshangar and J. Soleimani Rad, *Eur. Polym. J.*, 2019, **117**, 64–76.
5 Y. Okumura and K. Ito, *Adv. Mater.*, 2001, **13**, 485–487.
6 T. Murakami, B. V. K. J. Schmidt, H. R. Brown and C. J. Hawker, *Macromolecules*, 2015, **48**, 7774–7781.
7 Y. Noda, Y. Hayashi and K. Ito, *J. Appl. Polym. Sci.*, 2014, **131**, 40509.
8 K. Ito, *Polym. J.*, 2012, **44**, 38–41.
9 L. Ouyang, C. B. Highley, C. B. Rodell, W. Sun and J. A. Burdick, *ACS Biomater. Sci. Eng.*, 2016, **2**, 1743–1751.
10 J. P. Gong, Y. Katsuyama, T. Kurokawa and Y. Osada, *Adv. Mater.*, 2003, **15**, 1155–1158.
11 Z. Gong, G. Zhang, X. Zeng, J. Li, G. Li, W. Huang, R. Sun and C. Wong, *ACS Appl. Mater. Interfaces*, 2016, **8**, 24030–24037.
12 Z. Deng, T. Hu, Q. Lei, J. He, P. X. Ma and B. Guo, *ACS Appl. Mater. Interfaces*, 2019, **11**, 6796–6808.
13 J. Wang, A. Chiappone, I. Roppolo, F. Shao, E. Fantino, M. Lorusso, D. Rentsch, K. Dietliker, C. F. Pirri and H. Grützmacher, *Angew. Chemie Int. Ed.*, 2018, **57**, 2353–2356.
14 H.-J. Li, H. Jiang and K. Haraguchi, *Macromolecules*, 2018, **51**, 529–539.
15 S. C. Grindy, R. Learsch, D. Mozhdehi, J. Cheng, D. G. Barrett, Z. Guan, P. B. Messersmith and N. Holten-Andersen, *Nat. Mater.*, 2015, **14**, 1210–1216.
16 D. E. Fullenkamp, L. He, D. G. Barrett, W. R. Burghardt and P. B. Messersmith, *Macromolecules*, 2013, **46**, 1167–1174.
17 Y. Lee, H. J. Chung, S. Yeo, C.-H. Ahn, H. Lee, P. B. Messersmith and T. G. Park, *Soft Matter*, 2010, **6**, 977–983.
18 P. Sun, H. Zhang, D. Xu, Z. Wang, L. Wang, G. Gao, G. Hossain, J. Wu, R. Wang and J. Fu, *J. Mater. Chem. B*, 2019, **7**, 2619–2625.
19 T. Zhao, M. Tan, Y. Cui, C. Deng, H. Huang and M. Guo, *Polym. Chem.*, 2014, **5**, 4965–4973.
20 W. E. Rudzinski, A. M. Dave, U. H. Vaishnav, S. G. Kumbar, A. R.

Kulkarni and T. M. Aminabhavi, *Des. Monomers Polym.*, 2002, **5**, 39–65.

21   G. Cai, J. Wang, K. Qian, J. Chen, S. Li and P. S. Lee, *Adv. Sci.*, 2017, **4**, 1600190.

22   Y. Zhao, Z. Li, S. Song, K. Yang, H. Liu, Z. Yang, J. Wang, B. Yang and Q. Lin, *Adv. Funct. Mater.*, 2019, **29**, 1901474.

23   G. Gerlach, M. Guenther, J. Sorber, G. Suchaneck, K. F. Arndt and A. Richter, *Sensors Actuators, B Chem.*, 2005, **111–112**, 555–561.

24   N. Annabi, A. Tamayol, J. A. Uquillas, M. Akbari, L. E. Bertassoni, C. Cha, G. Camci-Unal, M. R. Dokmeci, N. A. Peppas and A. Khademhosseini, *Adv. Mater.*, 2014, **26**, 85–124.

25   J. A. Hunt, R. Chen, T. van Veen and N. Bryan, *J. Mater. Chem. B*, 2014, **2**, 5319–5338.

26   J. Hoque, N. Sangaj and S. Varghese, *Macromol. Biosci.*, 2019, **19**, 1800259.

27   J. L. Drury and D. J. Mooney, *Biomaterials*, 2003, **24**, 4337–4351.

28   A. Pfister, R. Landers, A. Laib, U. Hübner, R. Schmelzeisen and R. Mülhaupt, *J. Polym. Sci. Part A Polym. Chem.*, 2004, **42**, 624–638.

29   Q. Lin, X. Hou and C. Ke, *Angew. Chemie Int. Ed.*, 2017, **56**, 4452–4457.

30   C. B. Highley, C. B. Rodell and J. A. Burdick, *Adv. Mater.*, 2015, **27**, 5075–5079.

31   P. Jiang, C. Yan, Y. Guo, X. Zhang, M. Cai, X. Jia, X. Wang and F. Zhou, *Biomater. Sci.*, 2019, **7**, 1805–1814.

32   W. Wu, A. DeConinck and J. A. Lewis, *Adv. Mater.*, 2011, **23**, H178–H183.

33   X. Liu, H. Yuk, S. Lin, G. A. Parada, T.-C. Tang, E. Tham, C. de la Fuente-Nunez, T. K. Lu and X. Zhao, *Adv. Mater.*, 2018, **30**, 1704821.

34   P. T. Smith, A. Basu, A. Saha and A. Nelson, *Polymer (Guildf).*, 2018, **152**, 42–50.

35   L. Li, P. Zhang, Z. Zhang, Q. Lin, Y. Wu, A. Cheng, Y. Lin, C. M. Thompson, R. A. Smaldone and C. Ke, *Angew. Chem. Int. Ed.*, 2018, **57**, 5105–5109.

36   A. Saha, T. G. Johnston, R. T. Shafranek, C. J. Goodman, J. G. Zalatan, D. W. Storti, M. A. Ganter and A. Nelson, *ACS Appl. Mater. Interfaces*, 2018, **10**, 13373–13380.

37   S. H. Lee, Y. Lee, S.-W. Lee, H.-Y. Ji, J.-H. Lee, D. S. Lee and T. G. Park, *Acta Biomater.*, 2011, **7**, 1468–1476.

38   G. A. Appuhamillage, D. R. Berry, C. E. Benjamin, M. A. Luzuriaga, J. C. Reagan, J. J. Gassensmith and R. A. Smaldone, *Polym. Int.*, 2019, **68**, 964–971.

39   A. Sabnis, M. Rahimi, C. Chapman and K. T. Nguyen, *J. Biomed. Mater. Res. Part A*, 2009, **91A**, 52–59.

40   I. Mironi-Harpaz, D. Y. Wang, S. Venkatraman and D. Seliktar, *Acta Biomater.*, 2012, **8**, 1838–1848.

41   C. G. Williams, A. N. Malik, T. K. Kim, P. N. Manson and J. H. Elisseeff, *Biomaterials*, 2005, **26**, 1211–1218.

42   K. Yue, G. Trujillo-de Santiago, M. M. Alvarez, A. Tamayol, N. Annabi and A. Khademhosseini, *Biomaterials*, 2015, **73**, 254–271.

43   C. Fan, L. Liao, C. Zhang and L. Liu, *J. Mater. Chem. B*, 2013, **1**, 4251–4258.

44   D. P. Nair, M. Podgórski, S. Chatani, T. Gong, W. Xi, C. R. Fenoli and C. N. Bowman, *Chem. Mater.*, 2014, **26**, 724–744.

45   I. R. Schmolka, *J. Biomed. Mater. Res.*, 1972, **6**, 571–582.

46   Y. L. Su, H. Z. Liu, J. Wang and J. Y. Chen, *Langmuir*, 2002, **18**, 865–871.

47   C. Bilici and O. Okay, *Macromolecules*, 2013, **46**, 3125–3131.

48   O. Okay, *J. Mater. Chem. B*, 2019, **7**, 1581–1596.

49   N. K. Pandit and D. Wang, *Int. J. Pharm.*, 1998, **167**, 183–189.

50   A. E. Rydholm, K. S. Anseth and C. N. Bowman, *Acta Biomater.*, 2007, **3**, 449–455.

51   J. Liu, H. Zheng, P. S. P. Poh, H. G. Machens and A. F. Schilling, *Int. J. Mol. Sci.*, 2015, **16**, 15997–16016.

Non-covalent   Direct-write   Thiol-Michael
hydrogel   3D printing   crosslinked hydrogel

PBS